Dynamic analysis of immune and cancer cell interactions at single cell level in microfluidic droplets

S. Sarkar,[1,a)] P. Sabhachandani,[1,a)] D. Stroopinsky,[2] K. Palmer,[2] N. Cohen,[1] J. Rosenblatt,[2] D. Avigan,[2] and T. Konry[1,b)]
[1]*Department of Pharmaceutical Sciences, Northeastern University, 360 Huntington Avenue, Boston, Massachusetts 02115, USA*
[2]*Beth Israel Deaconess Medical Center, Harvard Medical School, Boston, Massachusetts 02115, USA*

(Received 27 July 2016; accepted 29 September 2016; published online 12 October 2016)

Cell-cell communication mediates immune responses to physiological stimuli at local and systemic levels. Intercellular communication occurs via a direct contact between cells as well as by secretory contact-independent mechanisms. However, there are few existing methods that allow quantitative resolution of contact-dependent and independent cellular processes in a rapid, precisely controlled, and dynamic format. This study utilizes a high-throughput microfluidic droplet array platform to analyze cell-cell interaction and effector functions at single cell level. Controlled encapsulation of distinct heterotypic cell pairs was achieved in a single-step cell loading process. Dynamic analysis of dendritic cell (DC)-T cell interactions demonstrated marked heterogeneity in the type of contact and duration. Non-stimulated DCs and T cells interacted less frequently and more transiently while antigen and chemokine-loaded DCs and T cells depicted highly stable interactions in addition to transient and sequential contact. The effector function of $CD8^+$ T cells was assessed via cytolysis of multiple myeloma cell line. Variable cell conjugation periods and killing time were detected irrespective of the activation of T cells, although activated T cells delivered significantly higher cytotoxicity. T cell alloreactivity against the target cells was partially mediated by secretion of interferon gamma, which was abrogated by the addition of a neutralizing antibody. These results suggest that the droplet array-based microfluidic platform is a powerful technique for dynamic phenotypic screening and potentially applicable for evaluation of novel cell-based immunotherapeutic agents. *Published by AIP Publishing*. [http://dx.doi.org/10.1063/1.4964716]

INTRODUCTION

Immune cells are highly migratory and interactive, which distinguishes them from many other cell types in the body. The nature and duration of intercellular contacts between diverse immune subsets is precisely regulated to achieve key cellular outcomes such as differentiation, priming, and effector functions. Lymphocytes initiate contacts with antigen-presenting cells (APC) such as dendritic cells (DC) following random trajectories, chemokine gradients, or topographical cues.[1,2] Contact-based intercellular communication between T cells and DCs is critical for the development of adaptive immune response to a variety of pathogens as well as cancer cells.[3–5] These conjugates are extremely heterogeneous, lasting from minutes to hours depending upon cell maturity, activation, and the presence of antigen-major histocompatibility complex (MHC).[3,6] The motility of the cell types involved and the dynamic character of the interactions require a continuous tracking of the cell conjugates rather than end-point analyses.

[a)]S. Sarkar and P. Sabhachandani contributed equally to this work.
[b)]Author to whom correspondence should be addressed. Electronic mail: t.konry@neu.edu. Tel.: 617 373 2423. Fax: 617 373 8886.

Although the molecular mechanisms of immunological synapses have been characterized in the past,[7] there are few techniques that permit dynamic quantification of immune cell conjugation and analysis of effector functions in an integrated platform.

DC-T cell interactions have been studied *in vitro* by imaging in a two dimensional environment, for example, on slides, plates, and planar bilayers.[8,9] This approach does not allow a suitable control over interaction parameters such as the number of cells involved, homotypic vs. heterotypic interaction, and cell motility. Characterization of non-adherent cells is particularly challenging over long durations required to assess various interaction phases (e.g., serial, transient, and stable). Immobilizing T cells on antibody or receptor ligand conjugated surfaces could result in differential responses as cells may activate specific intracellular signaling cascades.[10,11] Furthermore, motility is a crucial aspect of T cell response as the recognition of antigen results in a stop signal to migrating T cells followed by an activation phase and, finally, recovery of motility.[12] Therefore, constraining T cells physically or chemically could be deterrent to their activity.

Microfluidic single cell analysis platforms provide a robust, highly sensitive, and precisely controlled alternative for dynamic characterization of a sequential cellular interaction.[13–16] Various strategies have been employed for cell pairing, including hydrodynamic trapping in constrained channels, high density arrays containing two-sided traps, serpentine microchannels combined with apertures, surface acoustic waves, microwells, and droplets.[16–23] The hydrodynamic arraying methods rely on differential fluid flow resistance to deliver two types of cells sequentially into traps, often using a three- or four step loading protocol to achieve cell pairing at high efficiency (∼70%–80%).[19,20,24] Microwells permit gravity-based sedimentation of cells into the holding sites, also using a two-step cell loading process to promote "one-to-one" heterotypic contact between the immune cells. While these platforms permit live cell analysis by microscopy, they typically impose a design constraint in that the trap or well must be similar to the cell dimension so as to maximize cell capture and retention.[24] Thus, cell motility is severely restricted. With notable exceptions,[25,26] most traps do not preclude drifting of non-adherent cells over time or cross-talk between neighboring cell pairs.[17,24] In contrast, microfluidic droplets[27,28] allow greater cell mobility and retain cell-secreted factors within picoliter volume emulsions, limiting communication between nearest neighbors while allowing interaction between the co-encapsulated cells.[29] Serial interactions between the same cell pair and multiple pairs can also be observed in the droplets by adjusting the initial density of the heterotypic cells, thereby mimicking the situation *in vivo* where one cell type may encounter multiple cells.

In this study, we investigated the functional responses of activated effector immune cells dynamically in a microfluidic droplet array. We co-encapsulated DCs with naïve T cells at ratios ranging from 1:1 to 1:4 with respect to both cell types and characterized various parameters of interaction. The generated droplets were stably docked in an integrated microarray, allowing us to track individual cells and cell conjugates over a period of several hours. Cells were monitored from the point of contact initiation to quantify conjugate duration, stability of contact, and sequential interaction. We observed a strong heterogeneity in DC-T cell conjugation irrespective of the activation status of DCs. Antigen (Ag)-loaded DCs demonstrated both transient and stable interactions, whereas nontreated DCs interacted at low frequency. We also detected serial encounters between the same DC-T cell pair. The downstream effector functions of activated T cells were modeled by assessing CD8+ T cell-mediated cytolysis of cancer cells. T cells induced either fast or slow target death and in specific instances a sequential contact with target cells. The T cell response was mediated by a direct contact as well as secretion of Interferon gamma (IFN-γ), which affected a subpopulation of the target myeloma cells.

MATERIALS AND METHODS

Microfluidic device fabrication and droplet generation

The microfluidic devices were fabricated in accordance with standard soft-lithography protocols.[29,30] The device used for co-encapsulation of two cell types in droplets consisted of two cell suspension inlets: one oil inlet and two outlets. Co-encapsulation of three cell types was

achieved by modifying the device to incorporate three cell inlets. Each inlet was connected to an individual syringe via Tygon Micro Bore PVC Tubing (0.010″ ID, 0.030″ OD, 0.010″ wall, Small Parts, Inc., FL, USA). The fluid streams incubated through the inlets converge to a droplet-forming T-shaped nozzle, which then leads to an array comprised of 10^3 droplet-docking sites. The interior of the polydimethylsiloxane (PDMS) device was made hydrophobic by injecting Aquapel glass treatment (Aquapel, Pittsburg, USA). After 15 min, Aquapel was eliminated by flushing with air. The syringes were operated by individual syringe pumps (Harvard Apparatus, USA) which were programmed to set flow rates at each inlet. The oil to aqueous flow rates were generally maintained at a ratio of 4:1 to obtain optimal droplet sizes. The oil phase consisted of Fluorinert® FC-40 (Sigma, St. Louis, MO) supplemented with 2% w/w surfactant (008-FluoroSurfactant, Ran Biotechnologies, Beverly, MA). Droplet volume was assessed over a 10 h period and was found to vary by 5% ± 1.3%.

Cell isolation and culture

RPMI-8226 (multiple myeloma (MM) cell line) was purchased from the American Type Culture Collection (ATCC, Manassas, VA). CD8+ T cells were purchased from AllCells (#PB009-3F, AllCells, Alameda, CA). Cells were maintained in RPMI-1640 medium supplemented with 10% Fetal Bovine Serum and 1% Antibiotic-Antimycotic solution (Corning Cellgro, Manassas, VA). All cells were grown at 37 °C under 5% CO_2 in a humidified atmosphere. Cells were routinely passaged every three days and harvested at a density of 1×10^6 viable cells/ml. The isolated mature dendritic cells and naïve T cells were prepared as discussed previously.[31] Commercially available leukopaks obtained from healthy donors were used to isolate peripheral blood mononuclear cells (PBMCs) via Ficoll density gradient centrifugation. RPMI 1640 complete medium was prepared using heat inactivated 10% human AB male serum (Sigma, St. Louis, MO), 100 U/ml penicillin, and 100 μg/ml streptomycin (Mediatech, Herndon, VA), and 2 mM L-glutamine (Mediatech). PBMCs were incubated in this RPMI complete medium for 1 h at 37 °C. The non-adherent T cellrich population was removed by aspiration and labeled with anti-CD3 antibody. CD3+ T cells were sorted via flow cytometry and cryopreserved. The adherent fraction was cultured with granulocyte macrophage colony-stimulating factor (GM-CSF, 1000 U/ml, Berlex, Wayne/Montville, NJ), and interleukin-4 (IL-4, 1000 U/ml, R & D Systems, Minneapolis, MN) supplemented complete media for a period of 5 days to differentiate into immature DC populations. The DCs were further matured by treating them with 25 ng/ml TNFα for an additional 2 days. Expression of DC costimulatory and maturation markers (CD86 and/or CD83) was assessed by flow cytometric analysis.

Cell viability studies

Cell viability in droplets was determined by incorporating the Live/Dead Viability/Cytotoxicity assay reagents in droplets (Life Technologies, Carlsbad, CA). The final concentration of calcein AM (live cell indicator) and ethidium homodimer-1 (EthD-1, dead cell indicator) was maintained at 2 μM and 4 μM, respectively. Calcein AM was detected by time-lapse microscopy at excitation/emission: 494/517 nm. EthD-1 was read at 528/617 nm. The proportion of live cells was calculated as a ratio of the number of live cells to the total number of cells as expressed as "percentage viability."

Differential cell labeling

Co-encapsulation studies were performed by labeling different cell types with fluorescent trackers including CFSE Cell Trace and CellTracker Red CMTPX according to manufacturer's instructions Life Technologies (Grand Island, NY). Briefly, CFSE stock solutions (5 mM) were prepared in dimethyl sulfoxide (DMSO) and used at a final concentration of 10 μM by diluting in 1× phosphate buffered saline (PBS). The cells were labeled for 15 min at 37 °C on a shaker (300 RPM). Excess labeling solution was removed by aspiration and the cells suspended in fresh growth media before use. Dye uptake was visualized using the fluorescein isothiocyanate

(FITC) filter (Ex/Em - 492/517 nm). CMTPX dye stocks were prepared at a concentration of 10 mM and used at a final concentration of 10 μM. The cells were labeled 45 min at 37 °C and visualized using a DsRed filter (Ex/Em - 577/602 nm). Cell nuclei were labeled with Hoechst at room temperature for 10 min.

DC activation and DC-T cell interaction in droplets

Dendritic cells (DCs) were stimulated with 100 μg/ml ovalbumin (OVA (323–339)) peptide conjugated with FITC (Anaspec, Fremont, CA) overnight.[32,61,62] The Ag-loaded DCs were washed twice to remove excess OVA-FITC from the solution prior to treatment with CCL21 for 2 h (25 ng/ml, Abcam Cambridge, MA). Untreated T cells were labeled with CMTPX tracker off-chip. To promote single cell encapsulation in droplets, all experiments were performed by incubating 1×10^6 cells/ml of each cell type through distinct inlets of the microfluidic platform. Control experiments were performed with untreated DCs and T cells suspended in complete growth media in the droplets. In experiments utilizing RPMI-8226 cells, the third cell type was labeled only with Hoechst to distinguish it from the other cells. In experiments where DC vaccines, T cells, and RPMI-8226 cells were co-encapsulated, EthD-1 was added to the media to indicate cell death following the heterotypic interaction.

T cell activation and T cell-target interaction in droplets

$CD8^+$ T cells were stimulated with 10 ng/ml phorbol 12-myristate 13-acetate (PMA, Sigma) and 1 μg/ml ionomycin (Sigma) for 4 h prior to incubation in droplets.[25] The cells were washed, and 1×10^6 cells/ml were incubated in the droplet device. For co-encapsulation experiments, calcein AM-labeled RPMI-8226 cells were incubated through the second inlet of the device at similar cell concentrations. Wherever required, anti-human Interferon gamma (IFN-γ) antibody (eBiosciences, San Diego, CA) was added to the RPMI-8226 cell suspension at 1:30 (v/v) ratio. Control experiments were performed by co-encapsulating unstimulated T cells and calcein AM labeled RPMI-8226 cells at equivalent concentration without the addition of IFN-γ antibody.

IFN-γ ELISA

IFN-γ secretion by CD8+ T cells were measured by Enzyme Linked Immunosorbent Assay (ELISA). T cells were stimulated with PMA/Ionomycin as described above at a concentration of 1×10^6 cells/ml. At various intervals, 50 μl of media was removed and frozen for analysis. Control samples were collected from untreated cells. Cell debris was removed by centrifugation. ELISA was performed using the Human IFN-γ Quantikine ELISA Kit (R & D Systems, Minneapolis, MN) as per manufacturer's instructions. Briefly, 100 μl of standard IFN-γ, control or stimulated cell culture supernatant were added to the antibody-coated microplate strips and incubated at room temperature for 2 h. The wells were washed thrice with the assay buffer. 200 μl of horseradish peroxidase conjugated IFN-γ antibody was added to each well for further incubation of 2 h. The wells were washed repeatedly and incubated with a combination of hydrogen peroxide and tetramethylbenzidine for 30 min. The reaction was stopped with 2N sulfuric acid and the plate read at 450 nm with a correction readout set to 540 nm.

Image acquisition, processing, and statistical analysis

The phase/fluorescent images of cells in droplets were captured using a Zeiss Axio Observer. Z1 Microscope (Zeiss, Germany) equipped with a Hamamatsu digital camera C10600 Orca-R2, 10–40× objectives and standard FITC/DAPI (4′,6-diamidino-2-phenylindole)/TRITC (tetramethylrhodamine isothiocyanate) filters. The microfluidic device containing cells co-encapsulated droplets was maintained in a humidified microscopic stage-top incubator at 37 °C and 5% CO_2 for the duration of the experiment. Automated time-lapse images were obtained every 5 min for a total period of 12–16 h. For experiments requiring 1:1 cellular interactions, we scanned the whole array (1000 sites) immediately after co-encapsulation and selected droplets containing one

heterotypic cell pair. The software was programmed to image these specific locations at stated intervals over time. Interactions between multiple cells of each type were assessed in the same way by identifying locations in the droplet array containing ratios >1:1. We detected 27% droplets with single cells and 10% with heterotypic cell pair at 1:1 ratio. Image processing and analysis was done with ImageJ (http://rsb.info.nih.gov/ij/), Microsoft Office Excel 2010, and Origin Pro software. Contact periods were defined as cells forming visible conjugates for at least two consecutive time points. All periods of association and dissociation were counted for each cell and represented as percentage of total cells analyzed. T cell-mediated cytolysis was assessed from the loss of Calcein AM fluorescence in target cells, indicating leakage due to membrane perforation. Cell death was confirmed also by morphological markers (blebbing, swelling, and rupture). All statistical analyses were performed using Student t test, and p value <0.05 was considered statistically significant. The data are represented as the mean ± standard error of mean (SEM) of three independent experiments. Distribution of dynamic parameters, such as contact time and killing time, is represented as box-plots indicative of median, 25% and 75% quartile and outliers.

RESULTS

Microfluidic device design and cell co-encapsulation

The schematic of the integrated droplet generation and docking microfluidic platform is shown in Fig. 1(a). The device consists of two perpendicularly oriented inlets for introducing heterotypic cell suspension in the aqueous phase and a channel for the oil phase.[29,30] Robust

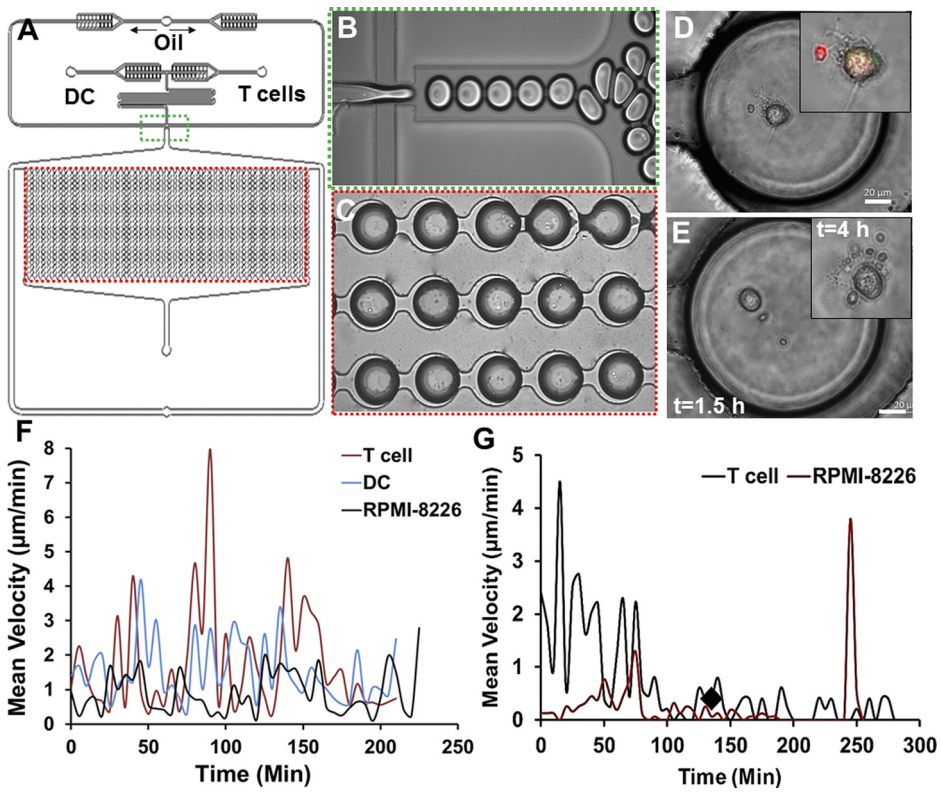

FIG. 1. Cell co-encapsulation in droplet microfluidic platform. (a) Schematic of integrated droplet generation and a microarray device. (b) Generation of nanoliter droplets. (c) Droplets loaded in a microarray for stable docking. (d) Morphology of single DC and T cell in the droplet. Inset: Magnified image of dendrite extension by DC. (e) Cellular exocytosis observed in the droplet. Inset: Magnified image of vesicles secreted by DC at 4 h. Scale bar: 20 μm. (F) Representative mean velocity profiles of one T cell, DC, and RPMI-8226 cell in the droplet. (g) A decrease in velocity as cells near each other and form conjugate. The onset of contact period is indicated by ◆. RPMI-8226 cell death occurred at 240 min and the complex dissociated rapidly.

monodisperse droplet generation was observed by shearing of an aqueous flow by oil at a flow-focusing zone (Fig. 1(b)). Consistent droplet sizes of ~100 μm diameter (i.e., 520 pl volume) were obtained by the optimization of flow rates of the two phases. The droplet generation junction is followed by a large docking array consisting of 10^3 trapping sites, where the droplets are stably arrested (Fig. 1(c)). We maintained the cell-encapsulated droplets for up to 24 h in a CO_2-rich and humidified atmosphere to improve cell viability.

Cell pairs (DC-T cells and T cells-cancer cells) were captured in the device through separate inlets in a single step loading process to ensure that interaction and activation occurred only in the droplets. A key advantage of our droplet docking platform is the ability to co-encapsulate cell pairs of different diameters, such as DCs and T cells, without optimization of trap geometry to match the cell dimension. Since the cells were not physically or chemically constrained, they were highly mobile inside the droplets, allowing us to track the cells from the point of contact initiation and conjugate formation. While a proportion of cells remained stably conjugated, the rest dissociated and underwent repetitive interactions. We quantified the dynamic parameters corresponding to continuous and intermittent interactions between cell pairs followed by effector functions (Fig. 2). We also monitored morphological changes such as dendrite extension by DCs (Fig. 1(d)) and vesicle release (Fig. 1(e)) by the cell pairs. In addition, all cellular secretions (e.g., cytokines) remain undiluted within the droplets, potentially leading to non-contact-mediated activation of co-encapsulated cells while minimizing stimulation of neighboring cells, which would not be possible with non-adherent cells in conventional culture conditions.

We tested the viability of various primary cells and cell lines in the droplets following individual and joint encapsulation.[25] T cells showed more than 90% viability in our droplet device. RPMI-8226 cells, a multiple myeloma (MM) cell line, depicted >75% viability in the droplets after 10 h (supplementary material Fig. S1). All viable cells depicted random motility within droplets. Periods of increased periods of velocity were observed (Fig. 1(f), supplementary

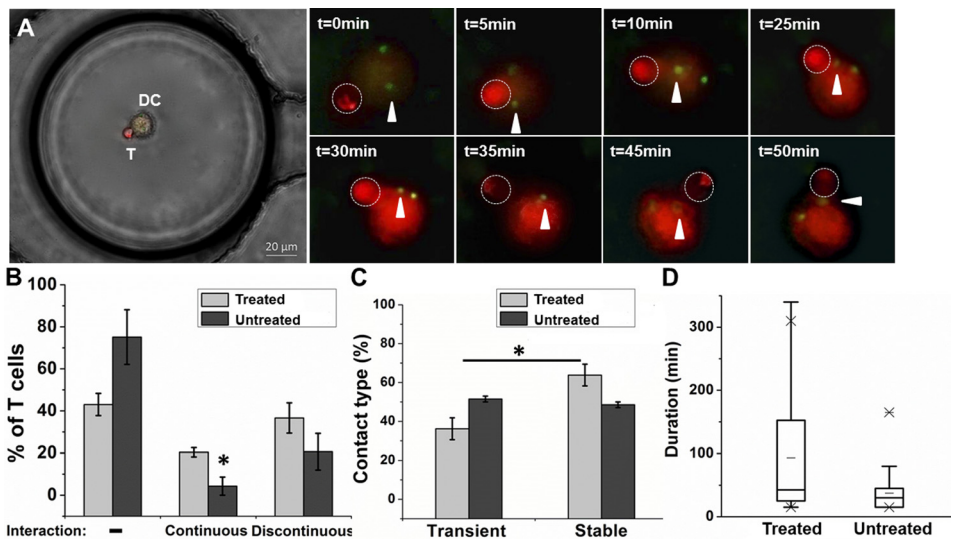

FIG. 2. Dynamic monitoring of interaction between stimulated DC and CD3+ T cells in microfluidic droplets. (a) DCs were pulsed with OVA-FITC (100 μg/ml, 16 h) and CCL21 (25 ng/ml, 2 h) and co-encapsulated with untreated T cells in droplets. OVA-FITC expression on the DC surface is indicated by arrowheads. T cells are labeled with CMTPX tracker (red), which is transferred to the DCs over time. A series of time-lapse images of the same droplet is shown over a period of 1 h. Images were obtained every 5 min. Scale bar: 20 μm. (b) Analysis of the types of interaction between DC and T cell: no interaction over a period of 5 h (-), continuous interaction for 5 h and discontinuous interaction defined by short periods of attachment and detachment. DCs were pre-treated with OVA-FITC and CCL21 (n = 227 cell pairs) or untreated (n = 100). (c) Cells undergoing a discontinuous interaction were further categorized into transient (≤10 min of contact) and stable (≥10min) interactions. (d) Distribution of contact times between DC and T cells (outliers are indicated). The data are represented as mean ± SEM of n = 3 independent experiments. $P < 0.05$ is indicated by *.

material Fig. S2), which decreased as cells moved closer and established contact with target cells (Fig. 1(g), supplementary material Fig. S3).

Dynamic profiling of immunological synapse and DC-T cell tracking

In this study, we investigated various aspects of T lymphocyte interactions to characterize heterogeneity in early stages of activation as well as later stages of effector function. We have shown previously that co-encapsulation of DCs with T cells in droplets results in reorganization of tubulin networks following physical contact between the cells.[29] The polarization of cytoskeletal components, including F-actin and tubulin, promotes active transport of signaling molecules, endocytosis, and receptor-mediated cellular communication at the immunological synapse.[33] Here, we characterized the initial interaction and dynamics of synaptic conjugation between DC and CD3+ T cells in the presence or absence of stimulating factors (e.g., chemokines and antigen). We also studied the late stage effector functions of T cells by co-encapsulating activated cytotoxic (CD8+) T cells with target cells in droplets.

Mature DCs that had not specifically been loaded with antigen (Ag) demonstrated relatively low interaction with non-stimulated CD3+ T cells. Among the DC-T cell pairs co-encapsulated, $20.6\% \pm 8.7\%$ cells showed short periods of interaction while $75\% \pm 13\%$ did not interact at all (Fig. 2(b)).

Next, we investigated dynamic interactions of Ag-loaded DCs and naïve T cells at single cell resolution. DCs were exposed to FITC-conjugated OVA (323–329) peptides overnight, followed by the treatment with CCL21 chemokine[34] before co-encapsulation in droplets with naïve T cells (Fig. 2(a)). The presence of lymphoid chemokines such as CCR7 ligands CCL19 and CCL21 in the lymph node is known to regulate immune cell migration, maturation, and effector functions.[35,36] We observed a marked increase in the extent of the DC-T cell interaction upon activation compared to control conditions. Long-lasting immune complexes (persisting for $\geq$5 h; referred to as "continuous" interaction hereafter) were observed in $20\% \pm 2\%$ cells, ~five-fold increase compared to control cells (Fig. 2(b)). The dynamic analysis also revealed strong heterogeneity in cellular interactions with respect to DC-T cell conjugate formation. $36.63\% \pm 7.13\%$ of T cells interacted discontinuously and asynchronously (referred to as "discontinuous" interaction) with the co-encapsulated DCs, forming repeated short term contacts (Figs. 2(b) and 2(c)). Further analysis of these cells revealed that the cells underwent transient or stable interaction. The transient interaction was defined by $\leq$10 min of cell complex retention; longer interactions were considered "stable." The discontinuous interaction was also observed between control DCs and T cells, although there was no statistical significance between transient and stable contacts among untreated DCs and T cells. However, stimulated DCs formed significantly greater stable conjugates with T cells (Fig. 2(c)). While the duration of the contacts varied from cell to cell, majority ($55.71\% \pm 3.72\%$) of the contacts lasted $\geq$40 min (Fig. 2(d)).

Reports indicate that *in vivo*, DCs demonstrate a significant motility towards CD3+ T cells irrespective of antigen presentation, although the migration trajectories are largely random.[41] Initial contacts between T cells and DCs were shown to be highly transient but antigen-loaded DCs made long-lasting contacts with T cells at 8–12 h after transfer in explanted lymph nodes.[37] Our data are in broad agreement with these findings[38] and also suggest that a combination of Ag and chemokine increases the frequency of contacts. The treated DCs formed both short- and long-lasting contacts ($>$100 min), and the duration of contacts was much longer compared to untreated DCs.

While immune cells are highly motile prior to forming complexes, cell movement ceases, or decreases significantly during interaction.[3,12] However, some motility exists within the complex itself, and T cells are known to spread out over APCs.[39,40] The conjugated cells in droplets showed lateral movement, in that the respective positions of the T cells on the surface of the DCs changed with time. The location of contact between the T cell and DC, shown in Fig. 2(a), shifted to a site bearing the OVA-FITC peptide at 50 min. This lateral motility of T cells was observed in all T-DC conjugates. DCs continually extended dendrites and pseudopods prior

to contact with T cells in droplets. Morphologically, the majority of contacts with T cells occurred on the DC cell body and not on dendrites, as reported in an intact lymphatic tissue.[41]

In the lymph nodes, DCs scan T cells at a rapid pace in a largely random manner.[41] In an effort to model this process in droplets, we increased the initial cell density of the two populations and observed interaction between multiple cells (Fig. 3). We found that a single DC could interact with more than one T cell simultaneously but not vice versa. It has been shown previously that both T cells and APCs can form "polygamous" conjugates *in vitro* and *in vivo*.[38,41,42] Quantitatively, there was no significant difference in the dynamic interaction parameters (contact duration, type, and numbers) between individual cells undergoing direct contact at 1:1 ratio versus multiple cell encapsulation. However, we found some DCs to be more "reactive" than others when multiple DCs were encapsulated with T cells, as single T cells essentially interacted with one DC during the observation period (Fig. 3(a)). Two of the T cells remained conjugated with the DC, while the third cell dissociated but did not interact with the other DCs present in the droplet. Quantification of the number of contacts made between specific cell pairs at 1:1 ratio indicated that 50% of the T cells made one contact with DC; smaller fractions of cells made 2–8 contacts over a period of 5 h (Fig. 3(b)). This was observed in T cells encapsulated with all DCs irrespective of Ag-loading and chemokine exposure. Such multiple contacts are estimated to be the result of scanning motion between DCs and T cells. The intermittent synaptic communication and a sequential contact between T cells and APCs have been shown to activate T cells in liquid cultures and collagen matrices,[43,44] suggesting that the dynamic interactions occurring in droplets could result in immune cell activation.

Together, these data demonstrate the heterogeneity in the dynamic events occurring in immunological synapse formation and establishes the suitability of the droplet microfluidic platform in assessing spatiotemporal dynamic events during immune response.

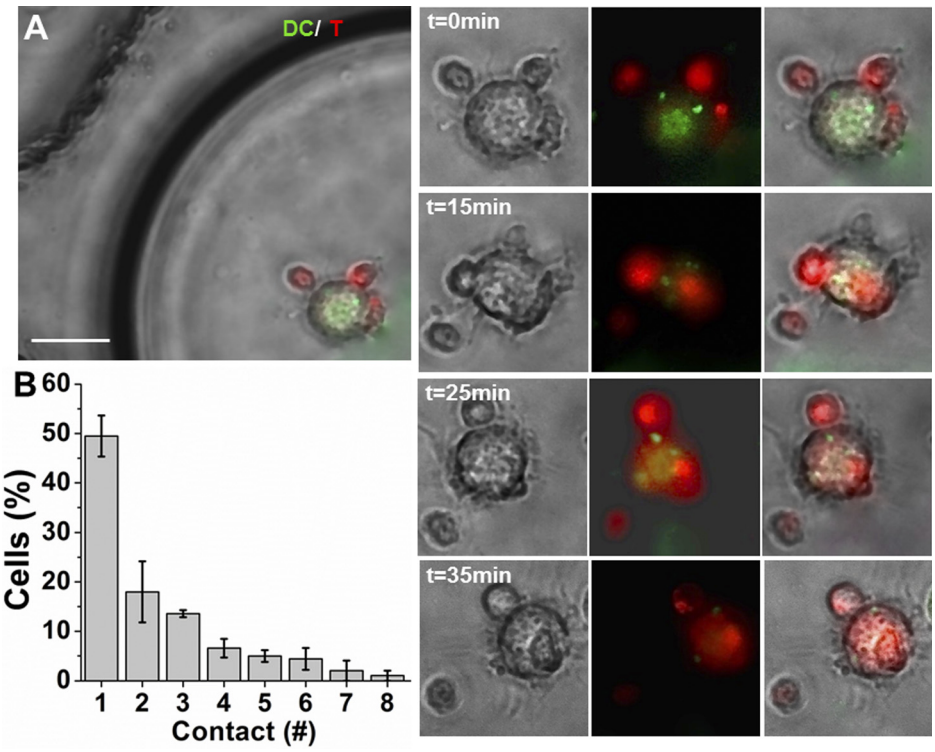

FIG. 3. (a) Interaction between multiple cells in droplets. DCs (green) were treated with OVA-FITC and CCL21. The CD3+ T cells were untreated and labeled with CMTPX (red) tracker. The panels (phase, fluorescent, and overlay) depict DC and T cells at various time points (representative of n = 30 droplets). Scale bar: 20 μm. (b) Number of contacts made between treated DC-T cell pairs (1:1 ratio). The data are represented as mean ± SEM from three independent experiments.

CD8$^+$ T cell-mediated cytolysis

Once activated, effector immune cells release cytokines, eliminate infected and transformed cells, and develop long-lasting memory cells. Effector immune functions rely heavily on competent CD8+ T cells, which can eliminate pathogen-infected host cells as well as cancer cells by exocytosis of cytotoxic granules, and activation of apoptotic pathways.[45,46] CD8+ T cells are capable of killing several target cells sequentially via rapid perforin upregulation and localization at the immunological synapse.[45] Here, we tested the feasibility of our device in assessing cancer cell killing by CD8+ T cells at an effector: target ratio of 1:1 (Fig. 4(a)). We used RPMI-8226 cells, a multiple myeloma (MM) cell line, as the target. Here, the allogeneic T cells are expected to react against foreign HLA (human leukocyte antigen encoding human MHC) molecules unlike in autologous cells where the T Cell Receptor (TCR) can recognize myeloma-associated antigens. However, autologous T cells from multiple myeloma patients are not readily available, and alloreactive cell-based antitumor therapeutics are currently under investigation in various cancer models.[47]

CD8+ T cells were stimulated in an antigen-independent manner by the addition of PMA/Ionomycin, which is known to increase cytokine secretion and promote synthesis of perforin.[25,45] We observed a significantly higher target cell death mediated by activated T cells

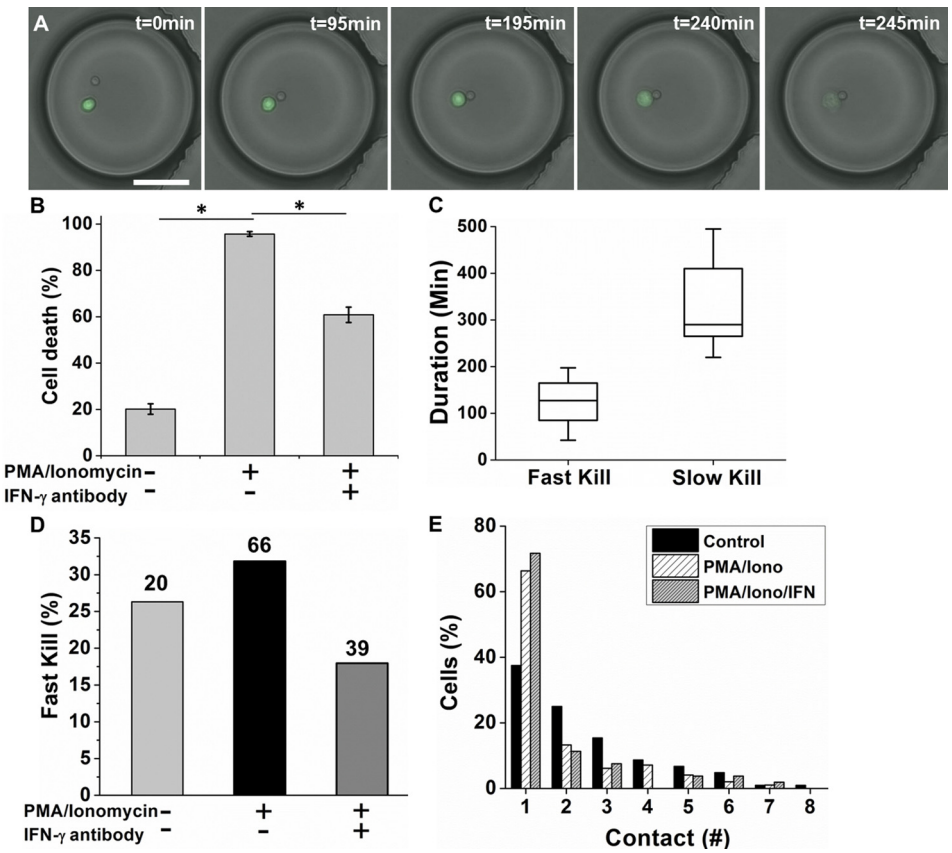

FIG. 4. Interaction between CD8+ T cells and target cells (RPMI-8226) in droplets. (a) Lysis and death of target cell in contact with CD8+ T cell. Target cells (green) were labeled with Calcein AM. Scale bar: 50 μm. The T cells were not labeled. (b) % of target cell death mediated by T cells (n = 3, mean ± SEM). $P < 0.05$ is indicated by *. A total of n = 292, 210, and 144 cells were quantified in Control, PMA/Ionomycin-treated, and PMA/Ionomycin/IFN-γ-treatment groups, respectively. (c) Comparison of time required by PMA/Ionomycin-treated T cells to promote target cell death. A threshold of 200 min was set for distinguishing fast vs. slow kill. (d) Effect of the presence/absence of IFN-γ antibody on rapid target death. Cell numbers (n) used for analysis in this representative experiment are indicated. (e) Number of contacts made between activated T cell-target cell pairs in a representative experiment. n: 104, 98, and 53 for Control, PMA/Ionomycin-treated, and PMA/Ionomycin/IFN-γ-treated cells, respectively.

compared with control T cells (95% vs. 20%) (Fig. 4(b)). Target death was verified by the loss of Calcein AM fluorescence,[30] indicating membrane damage as well as blebbing and a secondary membrane rupture. The duration of contact required for lysis and cancer cell death varied but mostly occurred after long-lasting, stable interactions. Two subsets of cellular phenotypes were identified based on killing times: fast and slow kill (Fig. 4(c)). However, limited number of cancer cells in control (7%) and stimulated categories (19.5%) were killed following transient contact (5–10 min). This suggests that T cell cytolytic activity is highly varied. Dynamic visualization of the same cell pair over several hours allowed us to determine the type of contacts initiated between the T cells and cancer cells. The majority (66%) of the activated T cells that came in contact with the target formed lasting complexes without further dissociation. In contrast, greater proportion (62.5%) of unstimulated T cells formed serial short-lived complexes with the target cell (Fig. 4(d)).

It has been shown previously that lethal amounts of perforin and granzyme can be released by T cells within seconds of contact, which can lead to apoptosis induction in 2 min.[48] However, the efficacy of the lytic hits is highly dependent on the species of the cytotoxic T lymphocytes as well as the type of target cells.[49,50] Interaction of Ag-specific T cells with target cells bearing the cognate Ag could potentially result in rapid synapse formation and faster accumulation of lytic granules at the synapse compared to non-specific T-target interaction. Additionally, heterogeneity in the T cell as well as RPMI-8226 population could also contribute to the differences in killing rates observed here. Primary MM cells and cell lines, including RPMI-8226, express carcinoembryonic antigen-related cell adhesion molecules that can inhibit CD8+ T cell activity *in vitro*.[51] We hypothesize that a combination of these factors regulated target cell death times in our study and could explain the differences in death times compared to previous reports.[48,49]

One of the hallmarks of T cell activation is the secretion of cytokines such as Interferon-gamma (IFN-γ) and Tumor Necrosis Factor-α (TNF-α).[25] We determined IFN-γ levels secreted by PMA/Ionomycin-stimulated CD8+ T cells (supplementary material Fig. S4). Addition of a neutralizing anti IFN-γ antibody in the droplets led to decreased target cell death (Fig. 4(b)). It primarily inhibited the "active" T cells mediating fast kills (Fig. 4(d)). IFN-γ has been shown to have paradoxical effects on cancer growth, providing both pro- and anti-tumorigenic signals.[50,52] IFN-γ is critical for antigen presentation and maturation but can induce T cell apoptosis and death of effector T cells.[53,54] Cytotoxic T cell responses are downregulated by IFN-γ in colon cancer.[55] Therefore, it is evident that the specific role of IFN-γ is highly contextual. Our findings suggest that IFN-γ contributes at least partially to RPMI-8226 cell death in droplets.

MM is characterized by significant clonal and mutational heterogeneity and remains incurable despite extensive efforts at development of novel therapeutic strategies.[56] The development of immunologic treatments to reverse tumor-mediated immune suppression and induce clinically meaningful anti-tumor immunity is a major area of research. These strategies include chimeric antigen receptor (CAR) T cells, DCs pulsed with tumor lysate and DC/tumor fusion cells capable of activating both helper and cytotoxic T lymphocytic responses.[57–59] The kinetics of activation, formation of immune synapse with the target cell, and cell killing by modified DC or T cells are still under investigation.[60] Our study suggests that the droplet microfluidics platform can be utilized to assess the dynamic response of cell-based vaccines in activating T cell effector functions against myeloma and other cancer cells.

CONCLUSION

In this study, we investigated the dynamics of live cell anti-tumor immune responses at the single cell level in a microfluidic platform. The integrated droplet array allowed improved control over heterotypic cell pairing and interactions, which allowed us to observe significant cell motility, morphological changes, and complex formation over an extended duration. We evaluated immune cell priming by Ag-loaded DCs and the subsequent functional outcome in the context of multiple myeloma cells. Our results demonstrate substantial heterogeneity in priming interactions between DC and T cells, both in basal and activated cells. Effector T cells depicted

time-varying cytotoxicity following transient, short or long stable contacts. Serial interactions by T cells were observed both in upstream (DC-based) and downstream (target-based) interactions. Our future aims include determining the molecular mechanisms underlying the phenotypic heterogeneity in T cell responses in droplets, and integrated live cell analysis of immune cell activation and effector functions. We anticipate that this platform could provide an insight into the behavioral response of novel cell-based immunotherapeutics such as chimeric antigen receptor T (CAR-T) cells and CAR-NK cells by phenotypic and functional analysis at single cell level.

SUPPLEMENTARY MATERIAL

See supplementary material for the demonstration of viability of RPMI-8226 cells in droplets, velocity profiles of T cells, RPMI 8226 cells, and Dendritic cells and secretion of IFN- γ by CD8+ T cells as measured by ELISA

ACKNOWLEDGMENTS

This work was funded by NIH/NCI Grant No. R21 [RM11-014] [to T.K.]. The authors are grateful to Abhinav Gupta, Vinny Motwani, and Sneha Verghese at Northeastern University for their assistance in fabrication of microfluidic devices and data analysis.

[1]D. M. Davis, Nat. Rev. Immunol. **9**, 543 (2009).
[2]J. B. Beltman, A. F. Marée, J. N. Lynch, M. J. Miller, and R. J. de Boer, J. Exp. Med. **204**, 771 (2007).
[3]P. Bousso, Nat. Rev. Immunol. **8**, 675 (2008).
[4]A. Lanzavecchia and F. Sallusto, Science **290**, 92 (2000).
[5]H. Salmon, K. Franciszkiewicz, D. Damotte, M. C. Dieu-Nosjean, P. Validire, A. Trautmann, F. Mami-Chouaib, and E. Donnadieu, J. Clin. Invest. **122**, 899 (2012).
[6]F. Benvenuti, C. Lagaudrière-Gesbert, I. Grandjean, C. Jancic, C. Hivroz, A. Trautmann, O. Lantz, and S. Amigorena, J. Immunol. **172**, 292 (2004).
[7]A. Grakoui, S. K. Bromley, C. Sumen, M. M. Davis, A. S. Shaw, P. M. Allen, and M. L. Dustin, Science **285**, 221 (1999).
[8]E. Woolf, I. Grigorova, A. Sagiv, V. Grabovsky, S. W. Feigelson, Z. Shulman, T. Hartmann, M. Sixt, J. G. Cyster, and R. Alon, Nat. Immunol. **8**, 1076 (2007).
[9]J. T. Groves and M. L. Dustin, J. Immunol. Methods **278**, 19 (2003).
[10]K. Shen, V. K. Thomas, M. L. Dustin, and L. C. Kam, Proc. Natl. Acad. Sci. U.S.A. **105**, 7791 (2008).
[11]Y. Kaizuka, A. D. Douglass, R. Varma, M. L. Dustin, and R. D. Vale, Proc. Natl. Acad. Sci. U.S.A. **104**, 20296 (2007).
[12]M. L. Dustin, S. K. Bromley, Z. Kan, D. A. Peterson, and E. R. Unanue, Proc. Natl. Acad. Sci. U.S.A. **94**, 3909 (1997).
[13]F. Guo, J. B. French, P. Li, H. Zhao, C. Y. Chan, J. R. Fick, S. J. Benkovic, and T. J. Huang, Lab Chip **13**, 3152 (2013).
[14]F. Guo, Z. Mao, Y. Chen, Z. Xie, J. P. Lata, P. Li, L. Ren, J. Liu, J. Yang, M. Dao, S. Suresh, and T. J. Huang, Proc. Natl. Acad. Sci. U.S.A. **113**, 1522 (2016).
[15]B. Dura, M. M. Servos, R. M. Barry, H. L. Ploegh, S. K. Dougan, and J. Voldman, Proc. Natl. Acad. Sci. U.S.A. **113**, E3599 (2016).
[16]S. Li, F. Guo, Y. Chen, X. Ding, P. Li, L. Wang, C. E. Cameron, and T. J. Huang, Anal Chem. **86**, 9853 (2014).
[17]P. J. Lee, P. J. Hung, R. Shaw, L. Jan, and L. P. Lee, Appl. Phys. Lett. **86**, 223902 (2005).
[18]S. Hong, Q. Pan, and L. P. Lee, Integr. Biol. **4**, 374 (2012).
[19]A. M. Skelley, O. Kirak, H. Suh, R. Jaenisch, and J. Voldman, Nat. Methods **6**, 147 (2009).
[20]J. P. Frimat, M. Becker, Y. Y. Chiang, U. Marggraf, D. Janasek, J. G. Hengstler, J. Franzke, and J. West, Lab Chip **11**, 231 (2011).
[21]F. Guo, P. Li, J. B. French, Z. Mao, H. Zhao, S. Li, N. Nama, J. R. Fick, S. J. Benkovic, and T. J. Huang, Proc. Natl. Acad. Sci. U.S.A. **112**, 43 (2015).
[22]Y. J. Yamanaka, C. T. Berger, M. Sips, P. C. Cheney, G. Alter, and J. C. Love, Integr. Biol. **4**, 1175 (2012).
[23]T. P. Lagus and J. F. Edd, RSC Adv. **3**, 20512 (2013).
[24]B. Dura, Y. Liu, and J. Voldman, Lab Chip **14**, 2783 (2014).
[25]Q. Han, N. Bagheri, E. M. Bradshaw, D. A. Hafler, D. A. Lauffenburger, and J. C. Love, Proc. Natl. Acad. Sci. U.S.A. **109**, 1607 (2012).
[26]Y. Lu, Q. Xue, M. R. Eisele, E. S. Sulistijo, K. Brower, L. Han, E. A. D. Amir, D. Pe'er, K. Miller-Jensen, and R. Fan, Proc. Natl. Acad. Sci. U.S.A. **112**, E607 (2015).
[27]T. Glawdel, C. Elbuken, and C. L. Ren, Phys. Rev. E **85**, 016322 (2012).
[28]F. Chen, Y. Zhan, T. Geng, H. Lian, P. Xu, and C. Lu, Anal. Chem. **83**, 8816 (2011).
[29]T. Konry, A. Golberg, and M. L. Yarmush, Sci. Rep. **3**, 3179 (2013).
[30]S. Sarkar, N. Cohen, P. Sabhachandani, and T. Konry, Lab Chip **15**, 4441 (2015).
[31]J. Rosenblatt, B. Vasir, L. Uhl, S. Blotta, C. MacNamara, P. Somaiya, Z. Wu, R. Joyce, J. D. Levine, D. Dombagoda, and Y. E. Yuan, Blood **117**, 393 (2011).
[32]B. J. McFarland, A. J. Sant, T. P. Lybrand, and C. Beeson, Biochemistry **38**, 16663 (1999).
[33]N. B. Martín-Cófreces, B. Alarcón, and F. Sánchez-Madrid, Front. Immunol. **2**, 24 (2011).
[34]R. S. Friedman, J. Jacobelli, and M. F. Krummel, Nat Immunol. **7**, 1101 (2006).

[35]B. J. Marsland, P. Bättig, M. Bauer, C. Ruedl, U. Lässing, R. R. Beerli, K. Dietmeier, L. Ivanova, T. Pfister, L. Vogt, and H. Nakano, Immunity **22**, 493 (2005).
[36]S. A. Luther, A. Bidgol, D. C. Hargreaves, A. Schmidt, Y. Xu, J. Paniyadi, M. Matloubian, and J. C. Cyster, J. Immunol. **169**, 424 (2002).
[37]T. R. Mempel, S. E. Henrickson, and U. H. Von Andrian, Nature **427**, 154 (2004).
[38]T. Okada, M. J. Miller, I. Parker, M. F. Krummel, M. Neighbors, S. B. Hartley, A. O'Garra, M. D. Cahalan, and J. G. Cyster, PLoS Biol. **3**, 150 (2005).
[39]P. Friedl, A. T. den Boer, and M. Gunzer, Nat. Rev. Immunol. **5**, 532 (2005).
[40]S. C. Bunnell, D. I. Hong, J. R. Kardon, T. Yamazaki, C. J. McGlade, V. A. Barr, and L. E. Samelson, J. Cell Biol. **158**, 1263 (2002).
[41]M. J. Miller, A. S. Hejazi, S. H. Wei, M. D. Cahalan, and I. Parker, Proc. Natl. Acad. Sci. U.S.A. **101**, 998 (2004).
[42]D. Depoil, R. Zaru, M. Guiraud, A. Chauveau, J. Harriague, G. Bismuth, C. Utzny, S. Müller, and S. Valitutti, Immunity **22**, 185 (2005).
[43]M. Faroudi, R. Zaru, P. Paulet, S. Müller, and S. Valitutti, J. Immunol. **171**, 1128 (2003).
[44]M. Gunzer, A. Schäfer, S. Borgmann, S. Grabbe, K. S. Zänker, E. B. Bröcker, E. Kämpgen, and P. Friedl, Immunity **13**, 323 (2000).
[45]G. Makedonas, P. P. Banerjee, R. Pandey, A. R. Hersperger, K. B. Sanborn, G. A. Hardy, J. S. Orange, and M. R. Betts, J. Immunol. **182**, 5560 (2009).
[46]B. Lowin, M. Hahne, C. Mattmann, and J. Tschopp, Nature **370**, 650 (1994).
[47]J. Arnason and D. Avigan, Immunotherapy **4**, 1043 (2012).
[48]J. A. Lopez, O. Susanto, M. R. Jenkins, N. Lukoyanova, V. R. Sutton, R. H. Law, A. Johnston, C. H. Bird, P. I. Bird, J. C. Whisstock, and J. A. Trapani, Blood **121**, 2659 (2013).
[49]J. A. Lopez, M. R. Jenkins, J. A. Rudd-Schmidt, A. J. Brennan, J. C. Danne, S. I. Mannering, J. A. Trapani, and I. Voskoboinik, J. Immunol. **191**, 2328 (2013).
[50]S. A. Ghanekar, L. E. Nomura, M. A. Suni, L. J. Picker, H. T. Maecker, and V. C. Maino, Clin. Diagn. Lab. Immunol. **8**, 628 (2001).
[51]M. Witzens-Harig, D. Hose, S. Jünger, C. Pfirschke, N. Khandelwal, L. Umansky, A. Seckinger, H. Conrad, B. Brackertz, T. Rème, and B. Gueckel, Blood **121**(22), 4493–4503 (2013).
[52]M. R. Zaidi and G. Merlino, Clin Cancer Res. **17**, 6118 (2011).
[53]A. Billiau, H. Heremans, K. Vermeire, and P. Matthys, Ann. N. Y. Acad. Sci. **856**, 22 (1998).
[54]V. Sobek, S. Balkow, H. Körner, and M. M. Simon, Eur. J. Immunol. **32**, 2490 (2002).
[55]G. L. Beatty and Y. Paterson, J. Immunol. **165**, 5502 (2000).
[56]R. Szalat and N. C. Munshi, Curr. Opin. Genet. Dev. **30**, 56 (2015).
[57]S. Guedan, X. Chen, A. Madar, C. Carpenito, S. E. McGettigan, M. J. Frigault, J. Lee, A. D. Posey, Jr., J. Scholler, N. Scholler, R. Bonneau, and C. H. June, Blood **124**, 1070 (2014).
[58]A. E. Chang, B. G. Redman, J. R. Whitfield, B. J. Nickoloff, T. M. Braun, P. P. Lee, J. D. Geiger, and J. J. Mulé, Clin. Cancer Res. **8**, 1021 (2002).
[59]M. R. Parkhurst, C. DePan, J. P. Riley, S. A. Rosenberg, and S. Shu, J. Immunol. **170**, 5317 (2003).
[60]A. J. Davenport, M. R. Jenkins, R. S. Cross, C. S. Yong, H. M. Prince, D. S. Ritchie, J. A. Trapani, M. H. Kershaw, P. K. Darcy, and P. J. Neeson, Cancer Immunol. Res. **3**, 483 (2015).
[61]J. M. Robertson, P. E. Jensen, and B. D. Evavold, J. Immunol. **164**, 4706 (2000).
[62]F. Spadaro, C. Lapenta, S. Donati, L. Abalsamo, V. Barnaba, F. Belardelli, S. M. Santini, and M. Ferrantini, Blood **119**, 1407 (2012).